Generation of non- thermal plasma jet using ZVS Driver with flyback transformer

Saba Mawlood Sulyman
University of Mosul
Basic Education College

Safa Aldeen Abdulla Sulyman
University of Mosul
Basic Education College

Abstract

The DBD plasma jet are generated using ZVS with flyback transformer, The equivalent circuit of ZVS driver was simulated by Multisim program, The data from simulation gave a good agreement with experimental data voltage, power and frequency . Furthermore, the electrical and optical properties of DBD plasma jet are obtained using analytical techniques, and it have been found that the system operates at voltages exceeding 9 kV, frequency 100 kHz and power of 5.67 Watts. Also, the measurement of reactive species produced in non-thermal plasmas NO and NOx with time are investigated. This jet was developed for medical applications and the effects of its emissions on microorganisms.

توليد نفاثة بلازما غير حرارية باستخدام مشغل ZVS مع محولFlyback

صفاء الدين عبدالله سليمان
جامعة الموصل
كلية التربية الاساسية

صبا مولود سليمان
جامعة الموصل
كلية التربية الاساسية

الملخص

تم توليد نفاثة بلازما DBD باستخدام مجهز القدرة ZVS مع محول flyback ، تم محاكاة الدائرة المكافئة لمحرك zvs بواسطة برنامج multisim ، وقد أعطت البيانات من المحاكاة توافقا جيدًا مع بيانات الجهد والقدرة والتردد. اضافة الى ذلك ، تم الحصول على الخواص الكهربائية والبصرية لنافث البلازما DBD باستخدام التقنيات التحليلية ، وقد وجد أن النظام يعمل بجهد تزيد عن 9 كيلو فولت ، وتردد 100 كيلو هرتز وقدرة 5.67 واط. كما تم دراسة قياس الأنواع التفاعلية المنتجة في البلازما غير الحرارية NO و NO_x مع مرور الزمن. تم تطوير هذا النفاث للتطبيقات الطبية وتأثيرات انبعاثاتها على الكائنات الحية الدقيقة.

---

*مستّل من رسالة ماجستّير الباحث الاول.

I. **Introduction**

 Plasma is one of the four basic states that make up 99% of the universe, which is considered a semi-neutral gas consisting of charged particles such as electrons, ions and neutral particles such as atoms. Plasma is divided into two types: thermal and non-thermal plasma, and it can be produced under low pressure or at atmospheric pressure and using a variety of energy sources. The non-thermal plasma is preferred for many applications due to its low temperature and flexibility of operation, such as in microbial purification or sterilization, medical treatment (Ehlbeck J. et al, 2011, Vesel A. and Primc G, 2020). Thus, It can be said that the efficiency and safety of cold plasma technology is suitable for biological and medical purposes There are many types of electrical discharge methods that are used to produce plasma, and one of these methods is DBD jet discharge. This type of discharge is considered one of the best methods of discharging because it works under atmospheric pressure, and at a temperature that does not exceed much from room temperature. Also, It is called silent discharge, and it is characterized by the use of parallel electrodes that operate using high alternating voltage, and the two electrodes are isolated from each other with an insulating material Thus, it is considered harmless for heat sensitive biological materials such as vital human tissues, it has been used as a treatment for tumors and skin diseases such as infections as well as clinical applications, for its antimicrobial properties (Wiegand C., 2019). There are some important parameters in the treatment of biological materials such as the duration of treatment and the distance between the sample and the tip of the plasma needle, value of the applied voltage and the amount of gas flow, In addition to the type of gas used, it is an important factor for the production of the active elements (Murbet H., et al, 2014). Plasma generation leads to the production of many active products including (ROS) and (RNS), which play an important role in biological materials such as the redox process (Keidar M., et al., 2013 and Lin Y., 2018). In this work, the DBD plasma jet was created using ZVS driver power supply. Also, The simulation of ZVS circuit are examined. Furthermore, the electric and optical properties as well as the measurement of reactive species produced in non-thermal plasmas NO and NOx are investigated.

II. **Experimental Setup of plasma system:**
 The plasma system consists of several parts that important to generation of non-thermal plasma under atmospheric pressure, which include the plasma needle, the inert gas (Helium gas), and the power source representing a high voltage bipolar pulse generator as shown in **Figure** 1.
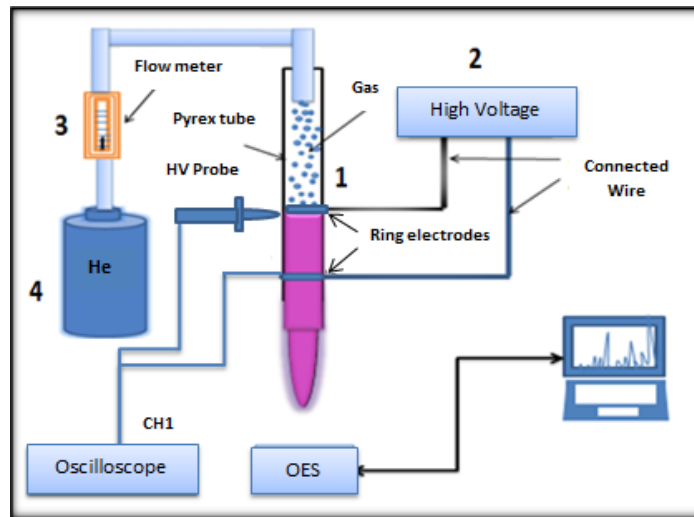
Figure 1. diagram of the plasma system

A. *Plasma needle:*

The plasma needle consists of a Pyrex tube with an outer and inner diameter (0.65, 0.5) mm respectively, helium gas passes through it and occurs the electric discharge. Discharge is using two copper electrodes, one of the electrodes is fixed inside a glass tube (anode), and the other around the tube from the outside. With a separation distance between the electrodes that can be controlled in a range of (4,5,6) cm when the gas started flowing (in proportions controlled by the flow meter) and the system was provided with high electrical power. As the gas begins to flow through the tube and provide the system with high electrical power, the gas molecules at the end of the needle tip are ionized as the gas mixes with the surrounding air at room temperature.
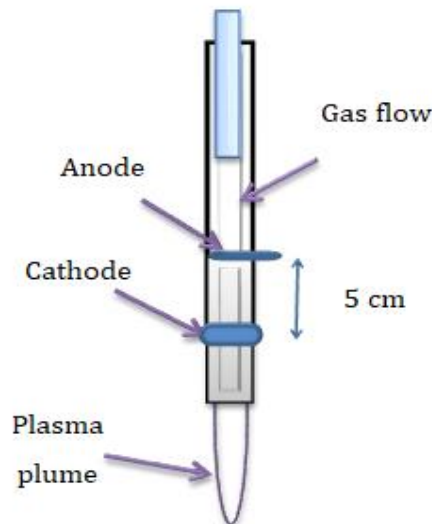
Figure (2) diagram of a plasma needle

B. *High Voltage Power Supply:*

The high voltage source that enables the system to generate plasma are made according to Mazzilli Circuit with slight modification (Zin R., et al., 2017), the high voltage circuit consists of an (ZVS) driver and Flyback transformer (provided from electronic store). The ZVS driver is a type of electrical circuit that generates high voltage at high frequency, The ZVS circuit operated by a low DC voltage (KN Corporation, Ireland). The Flyback transformer connects with an electrical circuit (ZVS) is type (FBT, model 20723, USA), to raise the high-frequency alternating voltage obtained from the circuit to a voltage high enough to enable the gas to ionize and reach the plasma state.

C. *Ionizing gas:*

In this study, helium gas was used for the purpose of the electric discharge process, with the possibility of controlling the gas passage for three gas flows (1, 2, 3) L/min respectively by using a flow meter (**KI, USA**) .

D. *The physical properties of plasma*

Several properties have been studied, including the analysis of the electrical properties of the plasma, by measuring the voltage at the electrodes using a high-voltage probe with high accuracy, which is connected to the oscilloscope. After connecting the two ends of the probe (**PINTECH, China**) with the electrodes of the system, the waveform is observed on the screen of the oscilloscope, and the voltage and frequency values are noted. Also, the value of the current was measured using a resistance (47 ohms), connected in series with the cathode electrode and using Ohm's law the value of the current was found, noting the waveform on the oscilloscope. Also, the electrical power of plasma system obtained using the following:

$$P = \frac{1}{T} \int_0^T I_d(t) V_g(t) \, dt$$

Where:

P: electric power
T: period of one cycle
I_d: Discharge current
V_g: gab voltage.

Furthermore, the spectroscopic diagnosis of plasma was also carried out using a Spectrometer (Model 77400, Spectro meter). In addition to Measurement the length of the plasma plume, which represents the distance between the tip of the plasma needle and the end of the jet, the distance was calculated using the usual ruler, the plasma temperature was measured using a digital thermometer with high accuracy that measures the temperature at different time intervals and for different gas flows .

III. **Simulation of electric circuit (ZVS and Flyback):**

Figure 3. shown The equivalent circuit was designed by National Instrument, version 14.0. According to (Vladimir Mazelli) of (ZVS) circuit and flyback driver using simulation software (Multisim) to generate high voltage to drive the plasma as in the study (Zin R., et al., 2017) with some changes. Using program helps to check results and monitor changes using multiple inputs that ensure the safty of the actual circuit. It represents a reformulation of the practical idea, but in an artificial and Similar way to natural conditions.
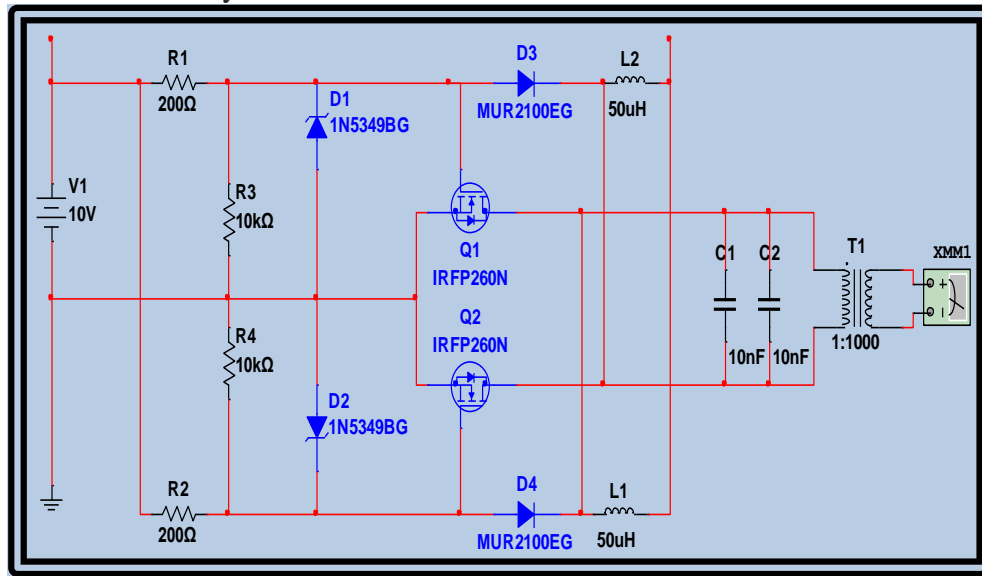
Figure 3. Electrical circuit of ZVS with flyback

All components of the electrical circuit were connected using the program, which consisted of two parts, the Flyback transformer and the driver circuit (ZVS). The basic principle of the design idea of this circuit is to charge a number of capacitors connected in parallel and then discharge them in series. The resonant inverter circuit consists of a pair of MOSFETs (IRFP260) and a pair of zener diode. When the circuit is applied with voltage, current flows on both sides of the MOSFET.One MOSFETS runs faster than the other, in which case one will cause one to work and the other to stop, and we will have a voltage that goes up and down sinusoidally. When Q1 is working, the voltage will be grounded and drained, while the voltage at source Q2 rises to a peak and then reverse during the half cycle and store in LC as voltage, Q2 drops to zero and the gate current is removed to Q1 and the voltage rises to Q1, switching MOSFETS occurs at the lowest induced power. The process is repeated in the second half of the cycle, L1 is placed in the circuit to reduce the peak current from inflation, i.e. acts as a throttle to increase the current, and R1 reduces the charging current to the gates to avoid excessive current that generates damage to the MOSFET. As for R3, it pulls the voltage to ground (Zin R., et al., 2017, Benabbas. M., et al., 2014), as well as zener diodes to regulate voltage.

The resonant frequency depends on the value of inductance and capacitance (Humud H. et al, 2012). as in the equation:

$$f = \frac{1}{2\pi\sqrt{LC}}$$

whereas:

　　　f: frequency in hertz (HZ)
　　　L: inductance in henry
　　　C: coil capacity, in farads

After operating the circuit and checking its operation using the measuring devices in the program, several values of the voltage were entered and the output values were read through the voltmeter and the frequency values through the oscilloscope, the results were recorded in a table.

IV. **Results and Discussion**

A. ZVS circuit simulation

　　　Table 1. Shows the input voltage values and the output results for voltage, current and frequency for each of the experimental at 1 L/min of gas flow and simulation method.

Table 1. Input and output values using simulation software and experimental method

V_{IN} (volt)	Simulation			Experimental			Power (watt)
	V_{out} (k volt)	I_{out} (mA)	F_{out}(KHZ)	V_{out} (k volt)	I_{out} (mA)	F_{out}(KHZ)	
10	8.87 kv	0.71	101.2	9	0.63	100	5.67
12	10.6 kv	1.1	101.3	9.5	0.74	100	7.03
14	12.6 kv	1.2	101.5	10	0.85	100	8.5
16	14.51 kv	1.4	99.7	10.5	0.95	100	9.97

Table 1. revealed that the data from the simulation and experimental methods provided a good agreement for the voltage , current, and frequency values.

V/Div= 5v

Time/Div = 20µs
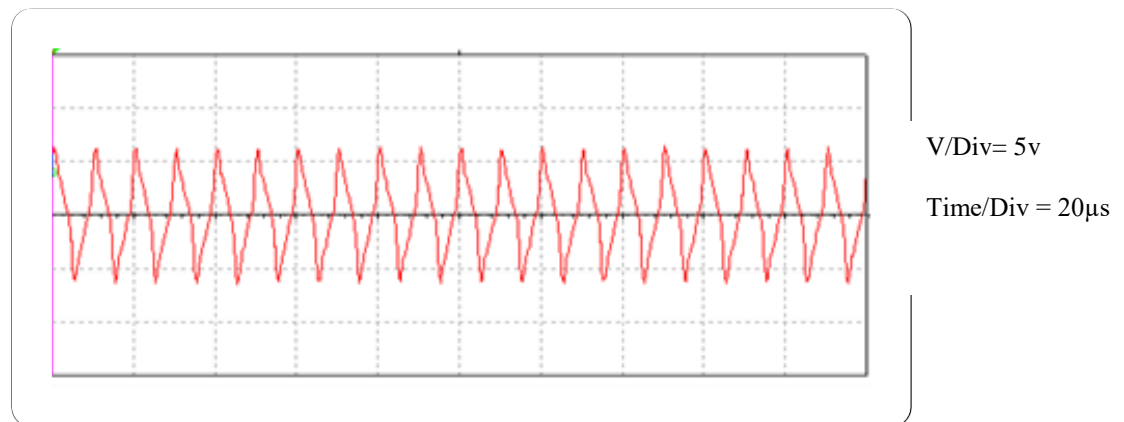
**Figure** 4. The waveform on the oscilloscope screen

Thus, the main objective of this paired circuit is to obtain a high voltage generator for the plasma system for the electrical discharge process, and this leads to a more stable circuit and higher output voltage (Muth'ah A. et al, 2020).

We note that the input voltage for this electrical circuit is a low constant voltage of several volts and supplied by a constant voltage source, but through the electrical circuit and the transformer produces a high output voltage (AC) . This circuit characterized by low loss (Xiaoyuan W. and Zhe Y ., 2012), Which included the LC resonant circuit, and the transformer with the ratio of N1:N2=5:1000. which that amplifies the input voltage in addition to improving the output voltage.

B. *Electrical properties*

The electrical properties include voltage and electric current, since the signal generated at high voltage was measured using an oscilloscope with a high voltage probe, and thus determined the amount of voltage that needed to ionize the gas and generation a plasma. As for the current meter it was calculated using Ohm's law.

The voltage required to generate the plasma was measured by using a special probe for high-voltage oscillations, and the waveform was observed using an oscilloscope and the pulse was as in **Figure** 5.

V/ DIV= 2.00 V

T / DIV= 5 µs

Probe = 1000 x
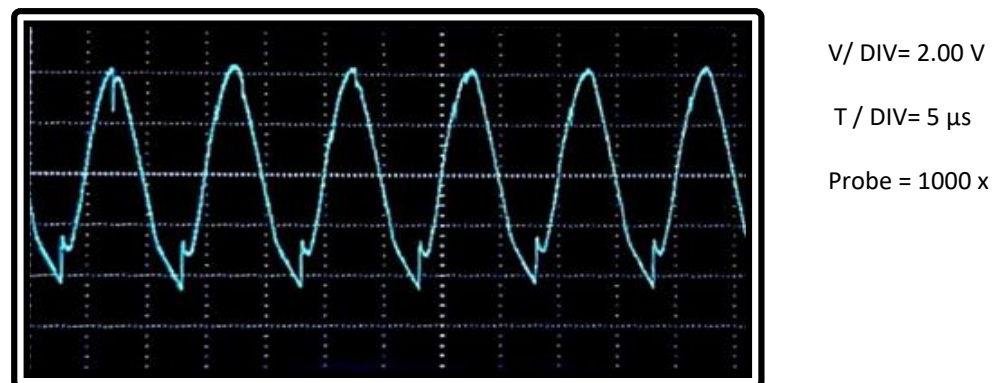
Figure 5. Plasma voltage waveform

The applied voltage between two electrodes, makes the electric field that generated in the gap transmitted to the plasma by accelerating the charge, the potential difference between the electrodes leads to the breakdown, with the electrons towards the positive electrode by the influence of the electric field, the gas atoms ionize and the number of electrons and the number of ions increases multiply (Fridman G. and Fridman A, 2011, Fu Wei et al., 2020). Generally, high energy is transfer by the electric field to the electrons and heavy molecules (gas molecules) due to ionization, excitation, separation, and elastic collisions. Elastic collisions between electrons and heavy particles predominate in the case of energy transfer in atomic gases. The transfer of energy from the electric field to the electrons is more efficient and more energy transfer than the case of energy transfer from electrons to heavy particles by collisions. This is because of the large difference in mass between electrons and heavy particles, , and for this reason the gas temperature is lower than the temperature of the electrons (Chu P. and LU X. , 2014). The output voltage was measured at different distances between the electrodes at a frequency of 100 kHz and the pulse shape from the oscilloscope screen as in **Figure** 5. was taken.

Table 2. The relationship between the plasma generation voltage and the distance between the electrodes

| (Distance between electrodes D (cm	(Inception Voltage (KV
4	8.5
5	9
6	9.5

By plotting the readings we got it from the graph as in **Figure** 6. we get the shape of the relationship between voltage and distance (D).
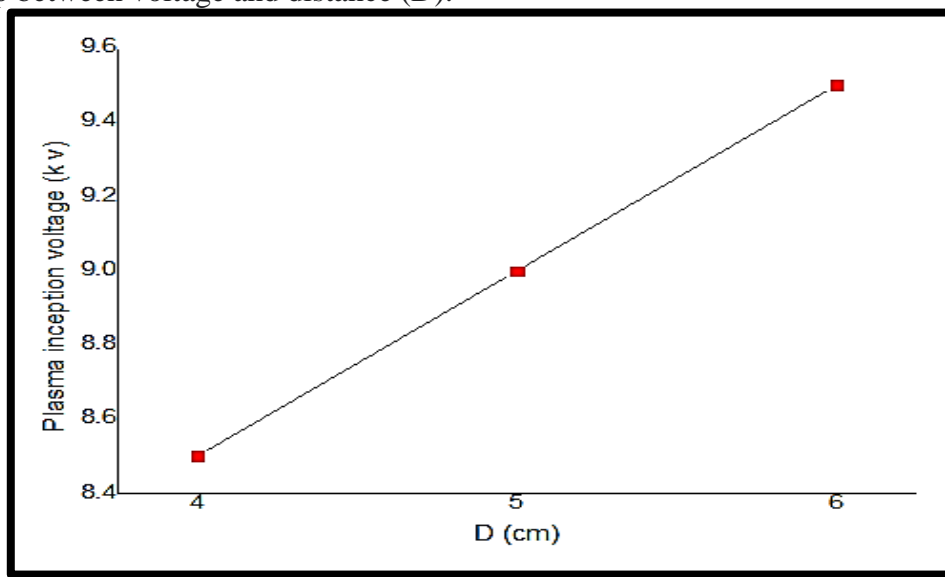
Figure 6. behavior of voltages with changing distance between electrodes

Figure 6. represents the relationship between the applied voltage and the distance between the electrods of the circuit. From this figure we can notice that increasing the distance of the electrodes leads to an increase in the voltage, which means that with this range of distances (4-6) the relationship between the distance between the electrodes and the voltage (Aldan M., 2015).

In order to learn more about the experimental properties of the plasma parameters, the instantaneous value of the electric current was recorded more accurately, the recorded pulses showed the shape of the pulse shown in **Figure** 7., where the voltage was measured from the figure and by applying Ohm's law R = V / I, the value of the current was estimated With 0.63 mA.


V/ Div = 10 mV

Time/Div = 10μs
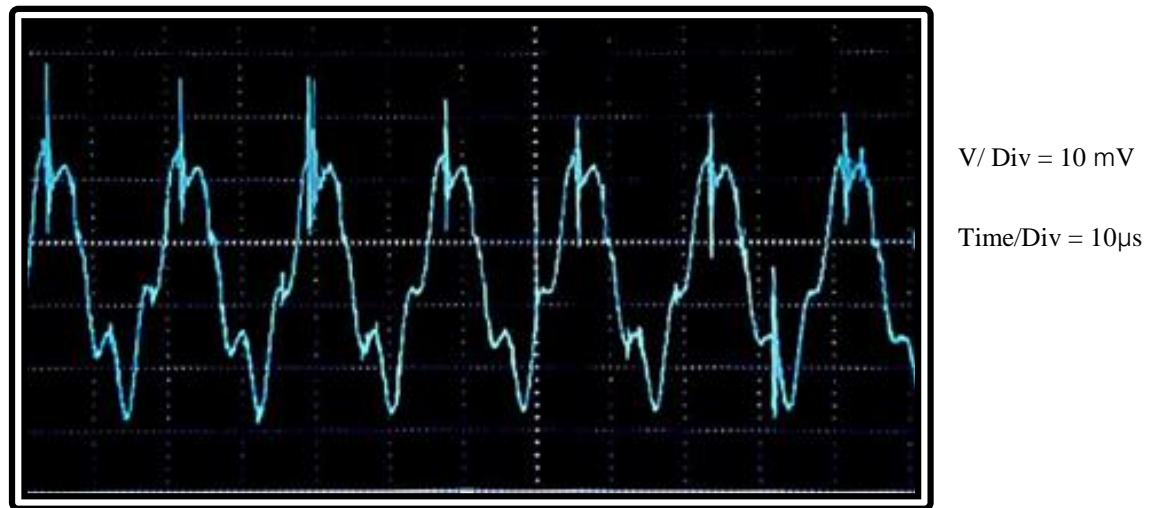
Figure 7. Output waveforms at the 47 Ω resistors

Increasing the input voltage leads to an increase in both the current and the output voltageThe ease of obtaining plasma voltage and current measurements gives a good advantage to plasmas, since most properties of the plasma generation system can be determined and characterized. The current was measured by calculating only the positive part of the sinusoidal voltage pulse, but the negative part of the pulse, the current is slight, and the results were corresponds with the study (Ohyama R. et al, 2009, Algwari Q., 2011), with the different gas use

c. *Optical properties*

In order to study the optical properties, a high-resolution optical spectrophotometer (OES) (ORIEL Model 77400 -USA) was used, and the element reactive produced after the formation of the plasma and the expulsion of gases outside the plasma needle were determined, within the range of the device used, where the emission spectra were recorded in the wavelength range of 400 to 900 nm, as shown in **Figure** (5).
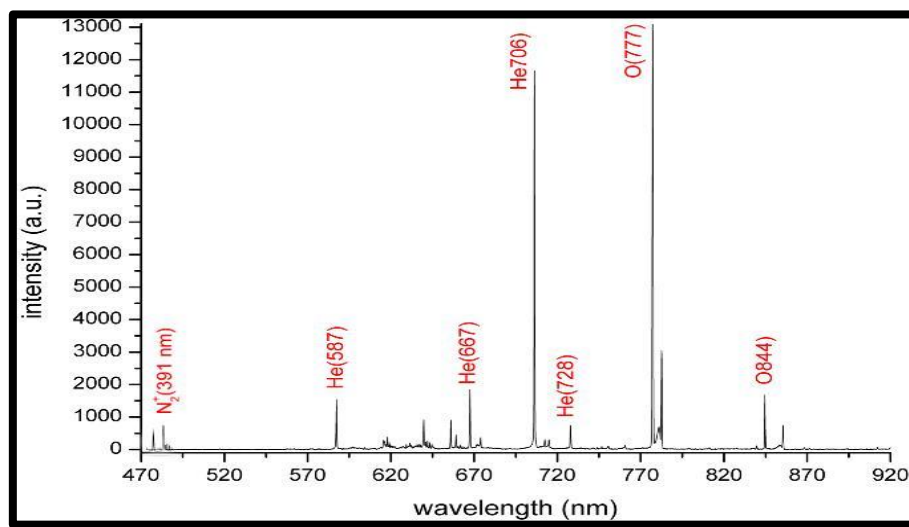
Figure 8. spectral intensity with wavelength

Figure 8. shows strong atomic lines for oxygen and helium, as well as a few lines for nitrogen in the visible spectrum. Element reactive are emitted into the air after the plasma is formed under atmospheric pressure, which is chemically active, and the electrons work to ionize and excite air molecules. The strongest emission was oxygen at the (777) nanometer line.

The production of a number of nitrogen and oxygen lines is one of the most effective factors affecting cells or organic matter in general. It was found that the intensity of the emission of these elements through the optical spectra depends on the intensity of the excited, the applied voltage, the emission characteristics (light, frequency, the probability of spontaneous emission and electric discharge), and the spectral response of the detection system, thus the emission intensity is a measure of element concentration for qualitative analysis. It was noted that the operating conditions by applying a higher voltage lead to a higher abundance in the production of reactive element. The evolution of electron density with flow rate must be taken into consideration (Bahnev B., 2011).

It should be noted that the measurements that were made were in the range (920-470) nm, and measurements of the UV range were not available, due to the limitation of the OES device that was used in the measurement. In the ultraviolet range, it was measured in a specific field of the electromagnetic spectrum, and no large proportions of gases were observed in the **Figure** 8. to measure the intensity of the spectrum. But after a period of operating the system and generating the plasma, a strong and widespread jet odor was observed, which indicates the production of abundant gases, such as the production of reactive oxygen species and reactive nitrogen species, which was confirmed using a device (gas analyzer) that measures the values of NO and NO_X for a period Adequate time which is recorded as in Table (5).

The reactive species generated include reactive oxygen species (ROS), reactive nitrogen species (RNS), ultraviolet radiation, active ions, and charged molecules. ROS may play the most important role in microbial inactivation (Joshi. et al., 2011). ROS is considered to have a strong oxidizing effect on microbes, which are all produced using plasma. As well as (RNS), which

works to significantly improve the chemical and microscopic properties of infected vital tissues. which can be easily developed by controlling the gas flow on the treated surface. The type and renge of the reactive element generated can influence the deactivation mechanism, and this range of interactive production may vary depending on the composition of the inert gas used (Shekhter A et al, 2005, Kuhn S et al, 2010).

D. *plasma plume length*

In Table 3., the change in plasma plume length with respect to helium gas flow rate for three different distances between electrodes (4, 5, 6).

Table 3. Shows gas flow values with the length of the plasma plume at the distances between the electrodes (4, 5, 6) cm

(D (cm	(Gas flow (L/min	(plume length(cm
cm 4	1	2.5
	2	4
	3	7.5
cm 5	1	3
	2	4.5
	3	8
cm 6	1	5. 3
	2	5
	3	9

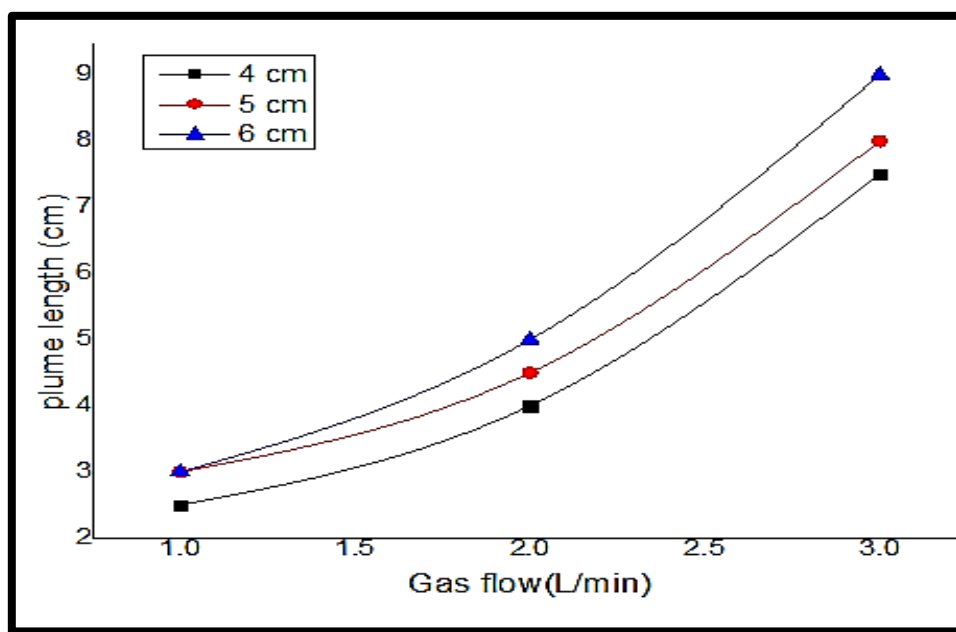These values are displayed graphically for each gas flow and for each electrode distance

Figure 9. the behavior of the length of the plasma plume as the gas flow changes for three different distances between the poles (4,5,6) cm.

Figure 9. shows one characteristic of the system, the effect of the gas flow rate on the length of the plasma plume on three different distances between the electrodes. It is clear from the **Figure** that the length of the plasma plume increases exponentially with the increase of the plasma flow. The maximum plasma plume length was 9 cm. This is due to the increased number of ionized atoms. As for the distance between the electrodes, it was observed that the change in the length of the shaft was slight (Al-Rawaf A et al., 2018).

E. *plasma plume temperature*

Another parameter of the plasma, the study of plume temperature with time change was measured by a microelectronic temperature sensor, and at multiple intervals (0-5) minutes and for three gas flows, as shown in Table (4).

Table (4) Change in plasma plume temperature over time with different gas flow values

(Time (min	Temp (C^O) (at 1(L/min	Temp (C^O) at (L/min) 2	Temp (C^O) at (L/min)3
0	25.5	25.5	25.5
0.5	26.8	26.7	26.6
1	27.4	27.3	27.1
2	28.1	27.7	27.4
3	28.5	28	27.7
4	28.8	28.3	27.9
5	29.1	28.5	28.1

The data in the above table for temperature is graphically illustrated for each time and for each gas flow.
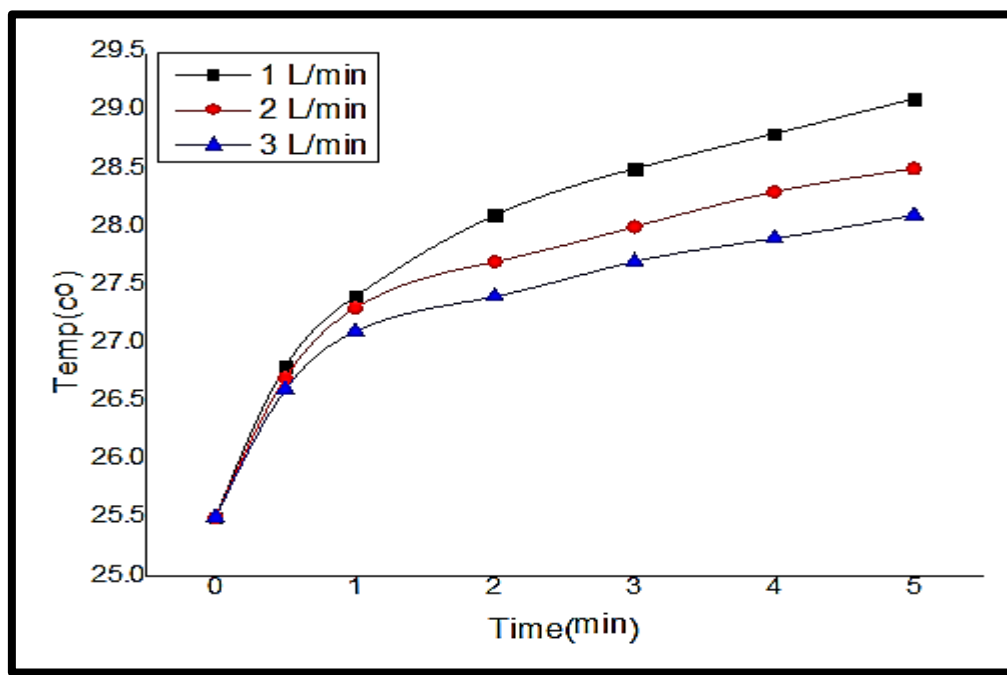
Figure 10. is the behavior of plasma temperature with time and for three gas flow states

Figure 10. shows slight increase in temperature over time with different plasma flow rates, but it was noted that this increase begins to be stable for all flow states before first minute and gradually with the continuation of the time period to reach the stable state, which represents a state of thermal equilibrium. In addition, the temperature decreases with the increase in the flow, and this is due to the high rate of collision of hot particles in the plasma plume with cold particles due to the increase in the flow of gas particles, which caused a decrease in the temperature of the plasma plume. This result indicates that the plume temperature can be effectively adjusted by controlling the gas flow rate. (AL-Rawaf A et al, 2018).

F. Plasma generation products

In addition to monitoring and controlling the spectral density of plasma products that containing a number of reacting products as in **Figure** 8., The concentration of one of the main products of the electrostatic discharge reaction (NO and NOx) was measured using gas analyzer (Model 330-2 L testo-Germany). Many concentration readings were recorded over time. The products (NO) reached up to 374PPM and NOx 376 PPM products within 10 minutes.

Table 5. represents the relationship between the concentrations of NO and NOx over time

Time (min)	(concentration (ppm	
	No	No$_x$
0.5	18	19
1	42	44
1.5	59	62
2	76	80
2.5	93	98
3	110	120
3.5	127	136
4	144	152
4.5	165	173
5	184	191
5.5	203	209
6	222	228
6.5	240	246
7	259	265
7.5	279	283
8	298	302
8.5	315	320
9	336	339
9.5	355	357
10	374	376

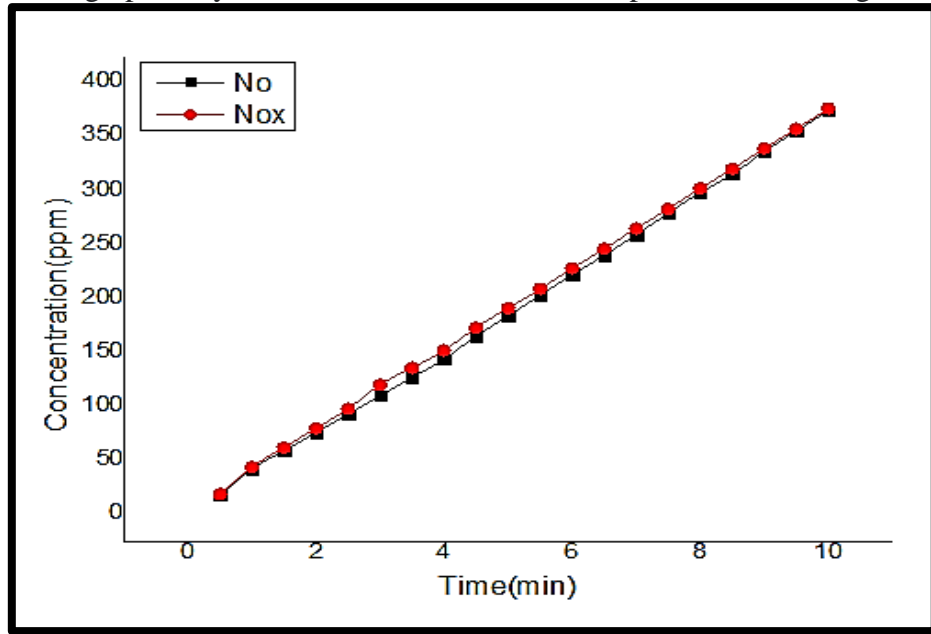Values are graphically illustrated for all NO and Nox production readings with time

Figure 11. The time evolution of NO and Nox.

Figure 11. shows the relationship between the concentrations of NO and NOx with time for a 9 kV DBD plasma system, measured using a (gas analyzer), and the measurements were taken to a duration of 10 minutes. It was observed that the concentration of nitrogen oxide was increasing and this increase with time is was linear. The relationship can be used to estimate the rate of nitrogen production. It is expected that in the case of a continuous increase over time, the linear shape changes due to the accumulation of the proportion of gas in the workplace (Pei X., et al., 2019).

The production of nitrogen oxides (RNS) using plasma discharge leads to a significant improvement in the chemical and microscopic properties of the affected biotissue (Dobrynin, D. et al., 2009). which can be easily developed by controlling the gas flow on the treated surface (Shekhter A et al, 2005, Kuhn S. et al, 2010). Making these measurements is very valuable for this gas because the element nitrogen is very important to plants, animals, and also humans and all living things on Earth. That is, plasma has an important role in the nitrogen cycle, so controlling all system conditions and measurements is important in this case to control the levels of NOx we produce. Plasma has become one of the most promising methods because of its many advantages discharge (Kuhn S. et al., 2010).

V. Conclusion

This research progresses in studying the characteristics of a non-thermal atmospheric pressure plasma jet designed by the DBD method. The electrical circuit of the power source was simulated, a number of voltage inputs were applied, the experimental results were compared with the simulation results, and with the study of the electrical and optical properties of the system, the behavior of the plasma plume with the change of gas flow and the distance between the electrodes, in addition to Studing the behavior of the plasma plume temperature over time, it showed The results are that the plasma was generated with a voltage of 9 kV, a power of 5.67 watts, and a frequency of 100 kHz. In addition to observing the spectral density of plasma products and calculating the concentration of nitrogen oxides, it was found that the simulation results with the practical results were very close, and the results also showed that the voltage is directly proportional to the increase in the distance between the electrodes and the electric field is inversely proportional to the distance, as well as the behavior of the plasma plume, Which obviously increases with increasing gas flow.

References

1- Aldan M. T. P., (2015), Modeling and Simulation of Electrical Breakdown in DC for Dielectric-Loaded Systems with Non-Orthogonal Boundaries Including the Effects of Space-Charge and Gaseous Collisions, University of California, Berkeley.

2- Algwari Q. T., (2011), PLASMA JET FORMATION AND INTERACTIONS BETWEEN ATMOSPHERIC PRESSURE DIELECTRIC BARRIER DISCHARGE JETS, MSc thesis, School of Mathematics and Physics, The Queen's University Belfast, 168.

3- AL-rawaf A., Khaddam F., Khalaf M., Oudah K., (2018), Studying the non-thermal plasma jet characteristics and application on bacterial decontamination, Theoretical and Applied Physics, 12, 45-51.

4- Bahnev B., (2011), Electrical and optical characterisation of an atmosphere pressure plasma jet and its interaction with plasmid DNA, PHD Thesis, The Open University, Department of Physics and Astronomy, 143.

5- Benabbas M.T., Sahli S., Benhamouda A. and Rebiai S., (2014), "Effects of the electrical excitation signal parameters on the geometry of an argon-based non-thermal atmospheric pressure plasma jet", Nanoscale Research Letters, 9, NO. 697.

6- Chu P. K., Lu X., (2014), Low Temperature Plasma Technology, Taylor & Francis Group, Boca Raton, FL, NO. 13, 33487-2742.

7- Dobrynin D., Fridman G., Friedman G. and Fridman A., (2009), Physical and biological mechanisms of direct plasma interaction with living tissue, New Journal of Physics, Vol. 11, 115020.

8- Ehlbeck J., Schnabel U., Polak M., Winter J., T., Brandenburg R., Von T., Hagen D., Weltmann K., (2011), Low temperature atmospheric pressure plasma sources for microbial decontamination, 44 (1), pp.13002.

9- Fridman G., Fridman A., and Brooks1A. D., (2011), Nonthermal Dielectric-Barrier Discharge Plasma-Induced Inactivation Involves Oxidative DNA Damage and Membrane Lipid Peroxidation in Escherichia coli, ANTIMICROBIAL AGENTS AND CHEMOTHERAPY, Vol. 55, No. 3, p. 1053–1062.

10- Fu Y., Zhang P., Verboncoeur J. P., Wang X., (2020), Electrical breakdown from macro to micro/nano scales: a tutorial and a review of the state of the art, IOP Publishing Ltd, Plasma Res Ex. 2 , 013001.

11- Humud H.R. , Wasfi A. S. , Abd Al-Razaq W., El-Ansary M. S., (2012), "Argon plasma needle source", Iraqe Journal of Physics, Vol. 10, NO. 17, PP. 53-57.

12- Joshi S. G., Cooper M., Yost A., Paff M. , Ercan U. K., Fridman G., , Fridman A. and Brooks A. D., (2011), Lipid Peroxidation in Escherichia coli Oxidative DNA Damage and Membrane Plasma-Induced Inactivation Involves Nonthermal Dielectric-Barrier Discharge, ANTIMICROBIAL AGENTS AND CHEMOTHERAPY, Mar., p. 1053–1062, Vol. 55, No. 3.

13- Keidar M., Shashurin A., Volotskova O., Stepp M., Srinivasan P., Sandler A., Trink B., (2013), Cold atmospheric plasma in cancer therapy, Phys. Plasmas 20, 057101-2.

14- Kuhn S., Bibinov N., Gesche R. and Awakowicz P., (2010), Non-thermal atmospheric pressure HF plasma source: generation of nitric oxide and ozone for bio-medical applications, Plasma Sources Sci. Technol, Vol. 19, 015013 (8pp).

15- Lin Y. T., (2018), "Enhancement of Selected Species in Nonthermal Atmospheric Pressure Plasma: Implications on Wound Healing Effects", IEEE Transactions on Plasma Science, 0093-3813.

16- murbet H. H., khadim Z. A., abdalameer N. K., (2014)" Effects of the small diameter and the flow rate on the electric properties of the plasma needle", IOSR Journal of Research & Method in Education (IOSR-JRME), e-ISSN: 2320–7388,p-ISSN: 2320–737X, Vol. 4, Issue 3 Ver. II, PP 81-84.

17- Muthi'ah A., Rahardjo A., Husnayain F., and Hudaya C., (2020), Design of Mazzilli's Zero Voltage Switching (ZVS) Circuit as Plasma Glow Discharge Generator, ELKHA , Vol. 12, No.2, pp. 112 – 118.

18- Ohyama R., Sakamoto M .and Nagai A., (2009), Axial plasma density propagation of barrier discharge non-thermal plasma bullets in an atmospheric pressure argon gas stream, J. Phys. D: Appl. Phys., Vol. 42 ,105203 (4pp).

19- Pei X., Gidon D., Yang Y-J., Xiong Z., Graves D. B. , (2019), Reducing energy cost of NOx production in air plasmas, Chemical Engineering Journal, Vol. 362, 217–228.

20- Shekhter A. B., Serezhenkov V. A., Rudenko T. G., Pekshev A. V., Vanin A. F., (2005), Beneficial effect of gaseous nitric oxide on the healing of skin wounds, Nitric Oxide, Vol. 12, 210–219.

21- Vesel A., Primc G., (2020), "Investigation of Surface Modification of Polystyrene by a Direct and Remote Atmospheric-Pressure Plasma Jet Treatment", Materials, Vol. 13, 2435.

22- Wiegand C., (2019), Potential of cold atmospheric pressure plasma (CAPP) in wound management, Wounds International, Vol 10 Issue 4.
Woodward S., (2015), E. coli bacteraemia: an overview, British Journal of Nursing, Vol 24, No 3.

23- Xiaoyuan W., Zhe Y., (2012), Simulation of ZVS Converter and Analysis of Its Switching Loss Based on PSPICE, International Journal of Power Electronics and Drive System (IJPEDS), Vol. 2, No.1, pp. 19~24.

24- Zin R. M., Soon C.F., Ab Sani M. Z., Rizon E. R., Tee K. S., Ahmad M. K., Ahmad N.N., Jubadi W. M., and Nayan N., (2017), "Zero voltage switching driver and flyback transformer for generation of atmospheric pressure plasma jet", AIP Conference Proceedings, vol. 1883, Issue 1, 020023.